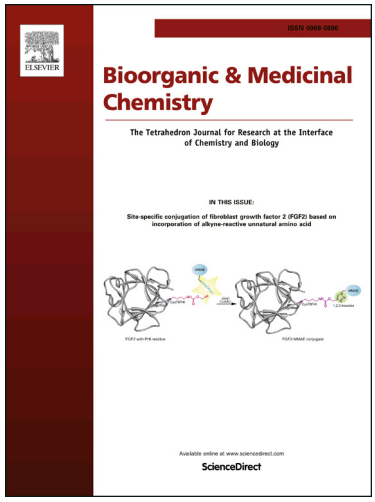

Synthesis and biological evaluation of fluoro-substituted 3,4-dihydroquinazoline derivatives for cytotoxic and analgesic effects

Jin Han Kim, Hui Rak Jeong, Da Woon Jung, Hong Bin Yoon, Sun Young Kim, Hyoung Ja Kim, Kyung-Tae Lee, Vinicius M. Gadotti, Junting Huang, Fang-Xiong Zhang, Gerald W. Zamponi, Jae Yeol Lee

PII: S0968-0896(17)30436-4
DOI: http://dx.doi.org/10.1016/j.bmc.2017.07.010
Reference: BMC 13846

To appear in: *Bioorganic & Medicinal Chemistry*

Received Date: 2 March 2017
Revised Date: 4 July 2017
Accepted Date: 6 July 2017

Please cite this article as: Kim, J.H., Jeong, H.R., Jung, D.W., Yoon, H.B., Kim, S.Y., Kim, H.J., Lee, K-T., Gadotti, V.M., Huang, J., Zhang, F-X., Zamponi, G.W., Lee, J.Y., Synthesis and biological evaluation of fluoro-substituted 3,4-dihydroquinazoline derivatives for cytotoxic and analgesic effects, *Bioorganic & Medicinal Chemistry* (2017), doi: http://dx.doi.org/10.1016/j.bmc.2017.07.010

Synthesis and biological evaluation of fluoro-substituted 3,4-dihydroquinazoline derivatives for cytotoxic and analgesic effects

Jin Han Kim [a, 1], Hui Rak Jeong [a, 1], Da Woon Jung [a], Hong Bin Yoon [a], Sun Young Kim [a], Hyoung Ja Kim [b], Kyung-Tae Lee [c,*], Vinicius M. Gadotti [d], Junting Huang [d], Fang-Xiong Zhang [d], Gerald W. Zamponi [d,*], Jae Yeol Lee [a, e,*]

[a] *Research Institute for Basic Sciences and Department of Chemistry, College of Sciences, Kyung Hee University, Seoul 02447, Republic of Korea*

[b] *Molecular Recognition Research Center, Future Convergence Research Division, Korea Institute of Science and Technology, Seoul 02792, Republic of Korea*

[c] *Department of Life and Nanopharmaceutical Science, Kyung Hee University, Seoul 02447, Republic of Korea*

[d] *Department of Physiology and Pharmacology, Hotchkiss Brain Institute and Alberta Children's Hospital Research Institute, Cumming School of Medicine, University of Calgary, Calgary T2N 4N1, Canada*

[e] *KHU-KIST Department of Converging Science and Technology, Kyung Hee University, Seoul 02447, Republic of Korea*

[1] *The contributions of the authors are equal.*

Corresponding authors:

Tel. +82 2 9610860; Fax +82 2 9620860; e-mail: ktlee@khu.ac.kr

Tel. +1 403 220 8687; Fax +1 403 210 8106; e-mail: zamponi@ucalgary.ca

Tel. +82-2-961-0726; Fax +82-2-961-0443; e-mail; ljy@khu.ac.kr

Keywords: T-type calcium channel; 3,4-dihydroquinazoline; bioisostere; cytotoxic activity; inflammatory pain; liver microsomal stability

Abstract: As a bioisosteric strategy to overcome the poor metabolic stability of lead compound KYS05090S, a series of new fluoro-substituted 3,4-dihydroquinazoline derivatives was prepared and evaluated for T-type calcium channel ($Ca_v3.2$) block, cytotoxic effects and liver microsomal stability. Among them, compound **8h** (KCP10068F) containing 4-fluorobenzyl amide potently blocked $Ca_v3.2$ currents (>90 % inhibition) at 10 μM concentration and exhibited cytotoxic effect (IC_{50} = 5.9 μM) in A549 non-small cell lung cancer cells that was comparable to KYS05090S. Furthermore, **8h** showed approximately a 2-fold increase in liver metabolic stability in rat and human species compared to KYS05090S. Based on these overall results, **8h** (KCP10068F) may therefore represent a good backup compound for KYS05090S for further biological investigations as novel cytotoxic agent. In addition, compound **8g** (KCP10067F) was found to partially protect from inflammatory pain via a blockade of $Ca_v3.2$ channels.

1. Introduction

Calcium (Ca^{2+}) as a second messenger plays a vital role in cellular physiology and biochemistry, such as proliferation, differentiation, growth, cell death and apoptosis.[1-4] Thus, alterations in calcium signaling can cause defects in cell growth and are associated with certain types of cancer.[5-7] A number of research groups have suggested a potential role for voltage-activated Ca^{2+} channels, in particular T-type (Ca_v3), in the regulation of tumor growth and progression.[8-14] This T-type Ca^{2+} channel family (Ca_v3) contains three members: $Ca_v3.1$, $Ca_v3.2$ and $Ca_v3.3$.[15] A growing number of reports show that T-type Ca^{2+} channels are abnormally overexpressed in many types of human cancers compared to normal cells.[16-17] Therefore, T-type Ca^{2+} channel blockers can be regarded as new tools in cancer therapies.[18-19]

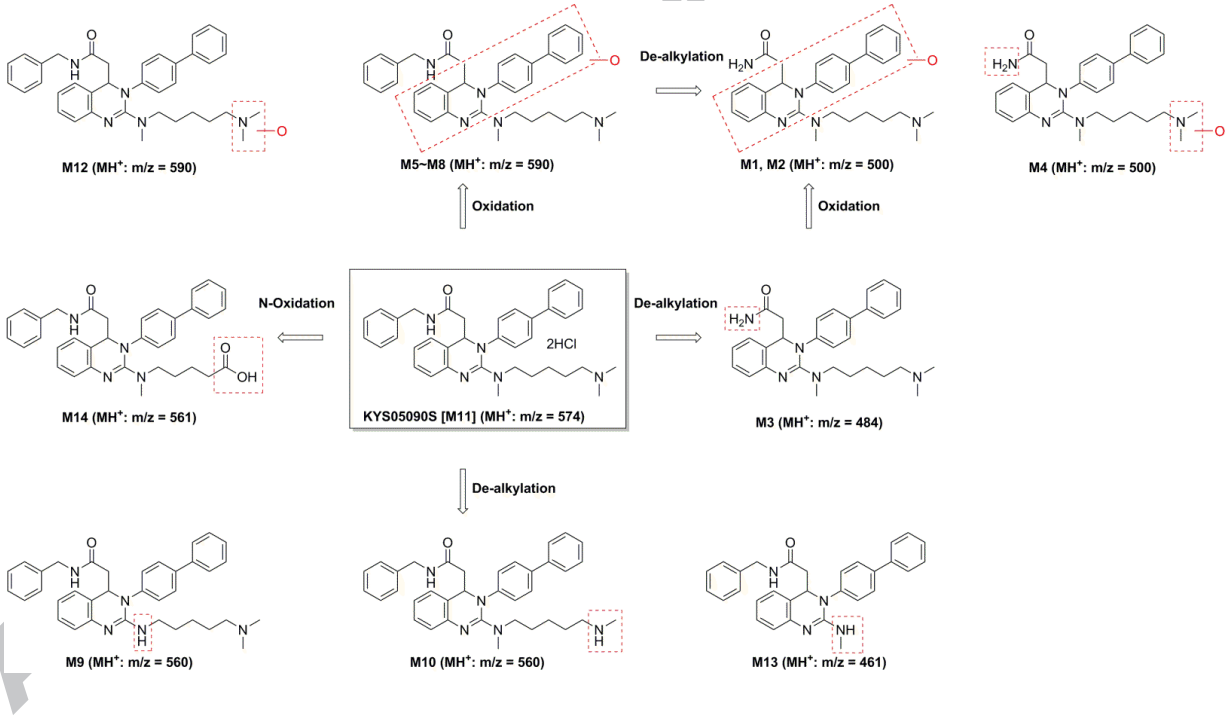

Figure 1. The proposed metabolic pathways and identified metabolites of KYS05090S in human, monkey, dog, rat and mouse liver microsomes.

We have already reported that 3,4-dihydroquinazoline derivatives exhibited both strong T-

type calcium blocking and anti-cancer effects.[20-25] An optimization study resulted in the lead compound KYS05090S for non-clinical studies.[26] We explored the *in vitro* metabolic stability of KYS05090S in mouse, rat, dog, and human liver microsomes using a single point metabolic assay.[27-28] Briefly, KYS05090S was incubated at a concentration of 1.0 μM with 1.0 mg/mL protein at 37 °C for 30 min. It showed lower metabolic stability with less than 30% remaining in liver microsomes of three species except dog (Table 1). *In vivo* pharmacokinetic (PK) studies of KYS05090S led to very low oral bioavailability in dog (*F*, 1.27%) and monkey (*F*, 2.01%) animals together with the formation of primary metabolites as shown in Fig. 1 (unpublished results).

Table 1. *In vitro* liver microsomal stability of KYS05090 [a]

Compound	% remaining after 30 min incubation			
	Human	Dog	Rat	Mouse
KYS05090S	16.6	> 100	24.2	27.6

[a] The metabolic stability was expressed as percent remaining compound after 30 minutes incubation in liver microsomal enzyme.

To overcome this issue, herein, we decided to insert a fluorine atom as a bioisostere of hydrogen atom into various regions of 3,4-dihydroquinazoline scaffold hoping that the small fluorine atom will not impair the binding of new synthetic 3,4-dihydroquinazoline derivatives to the target T-type Ca^{2+} channel. The rapid oxidative metabolism by the liver enzymes, in particular the P450 cytochromes, is often found to limit bioavailability. A frequently employed strategy to circumvent this problem is to block the reactive site by the introduction of a fluorine atom.[29] In fact, this bioisosteric strategy is one of the most commonly used methods for developing new compounds with improved pharmacodynamics and/or pharmacokinetic properties and thus has led to many successful drugs.[29-31]

2. Results and discussions

2.1. Chemistry

A series of fluoro-substituted 3,4-dihydroquinazoline derivatives (**8**) except **8f** in Table 2

was prepared using a Heck reaction (for **8d**and **8j**)[32] and the procedure described previously by our group.[20, 33] New compound **8f** (KCP10066F) was easily synthesized according to the procedure as shown in Scheme 1: Methyl 2-nitrocinnamate **1** was reduced with Zn (powder)/NH_4Cl into 2-aminocinnamate **2,** which was coupled with isocyanate (*in situ* prepared from 4-fluorobiphenyl-4-carboxylic acid **3** via Curtius rearrangement) to provide a urea **4**. The dehydration of **4** with $Ph_3P{\cdot}Br_2$ and Et_3N provided a carbodiimido **5**, which was subsequently coupled with piperazine compound **6** afforded 3,4-dihydroquinazoline ester **7**. The treatment of **7** with 5-fluorobenzylamine and 1,5,7-triazabicyclo[4.4.0]dec-5-ene (TBD) as a catalyst afforded the final compound **8f** (KCP10066F) under solvent-free condition.

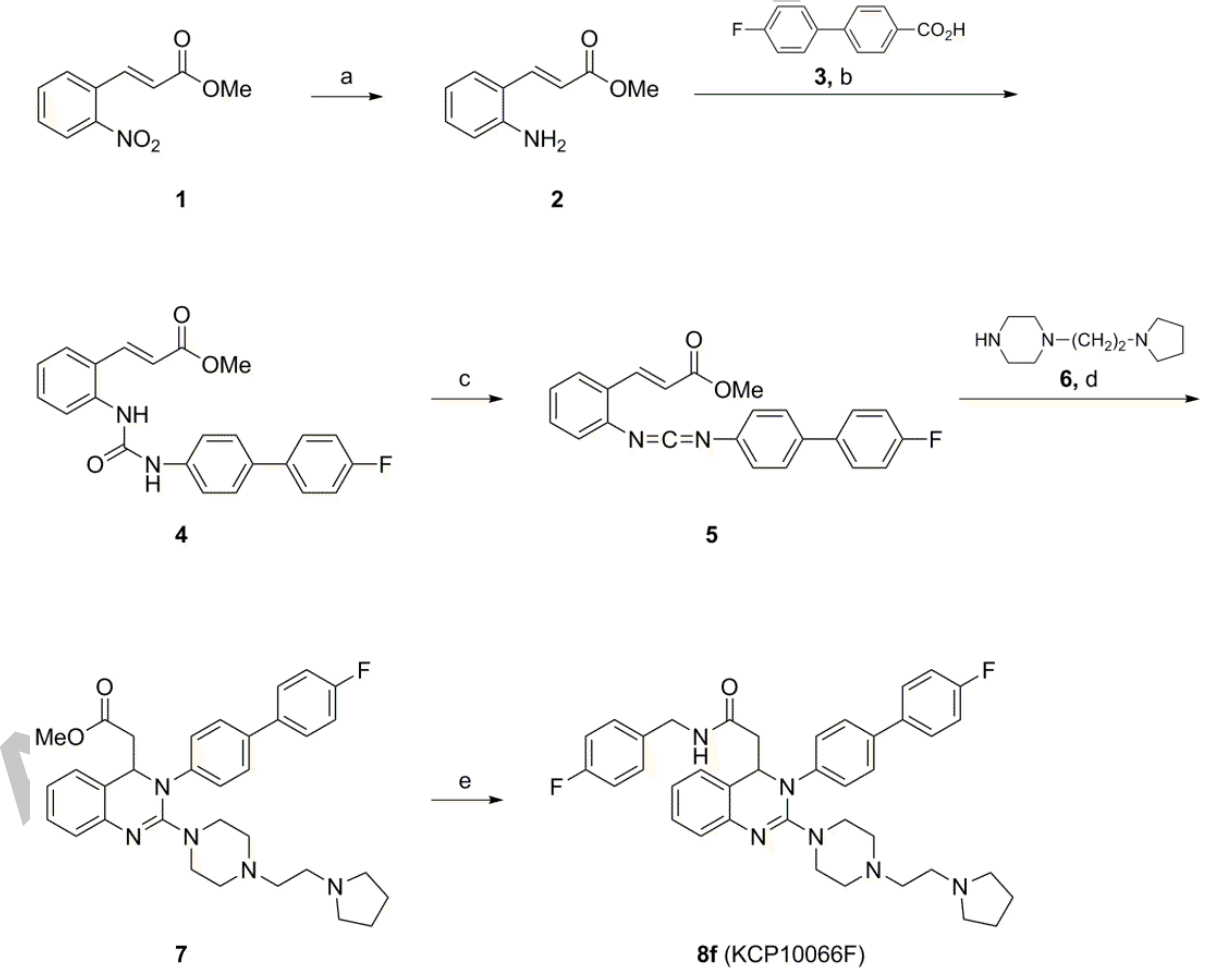

Scheme 1. Reagents and conditions: (a) Zn, NH_4Cl, MeOH, reflux, 12 h, 98%; (b) DPPA, Et_3N, toluene, rt to 100 ℃, 9 h, 54%; (c) $PPh_3{\cdot}Br_2$, Et_3N, CH_2Cl_2, 0℃, 12 h, 38%; (d) MeOH, rt, 4 h, 69%; (e) 4-fluorobenzylamine, TBD, 40 ℃, 12 h, 87%.

2.2. Biological evaluation

All compounds were tested for their abilities to block transiently expressed human $Ca_v3.2$ ($hCa_v3.2$) currents by using whole-cell patch clamp recordings in HEK cells.[34] Most of compounds except **8a** and **8f** potently blocked $Ca_v3.2$ currents (>90 % inhibition) at 10 μM concentration (Fig. 2A). Compound **8a** (KCP10048F) with a relatively short 4-isopropylphenyl ring at R^4 position was almost inactive, which was consistent with the reported result of SAR studies on the 3.4-dihydroquinazoline scaffold.[35] In contrast, compound **8d** (KCP10060F) and **8g** (KCP10067F) completely blocked $Ca_v3.2$ currents and their IC_{50} values determined from the fit to the dose-response curve were 5.6 and 5.1 μM, respectively, when cells were held at a hyperpolarized potential of -110 mV [Fig. 2C and 2D]. While the dose-response curve for compound **8d** could be fitted with a Hill coefficient of 0.8, that for compound **8g** required a Hill coefficient of 0.14. This suggests that block by **8g** required the interaction of more than one drug molecule with the channel and negative cooperativity. With respect to their channel selectivity, the two compounds showed poor $Ca_v3.2$ (T-type)/$Ca_v2.2$ (N-type) and (T-type)/$Ca_v1.2$ (L-type) calcium channel selectivity (Fig. 2B), suggesting that they are broad spectrum inhibitors of calcium channel activity.

Table 2. The biological activities of new synthetic 3,4-dihydroquinazoline derivatives (**8**)[a]

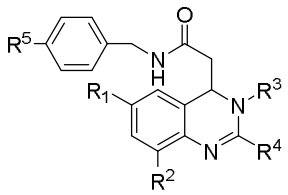

No	Code (KCP)	R^1	R^2	R^3	R^4	R^5	T-type ($Ca_v3.2$)[b,c]		A549[d]
							%inhibition	IC_{50} (μM)	IC_{50} (μM)
8a	**10048F**	H	H	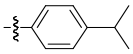	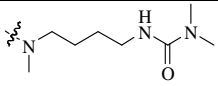	F	<10		5.7
8b	**10057F**	H	H	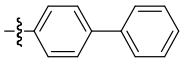	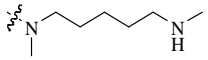	H	>90		8.7
8c	**10059F**	H	H	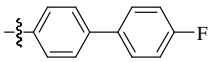	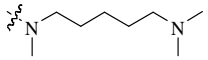	F	>90		2.2
8d	**10060F**	F	F	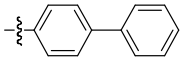	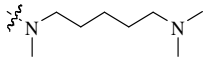	H	>95	5.6	5.1
8e	**10061F**	H	H	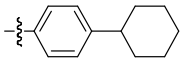	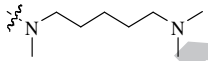	F	>90		7.1
8f	**10066F**	H	H	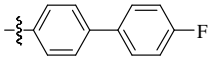	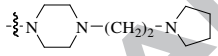	F	<80		8.7
8g	**10067F**	H	H	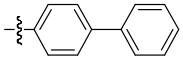	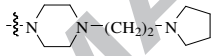	F	>95	5.1	7.6
8h	**10068F**	H	H	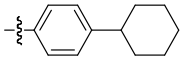	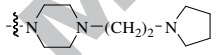	F	>90		5.9
8i	**10069F**	H	H	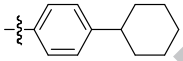	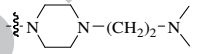	F	>90		5.9
8j	**10070F**	H	F	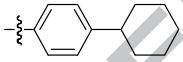	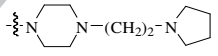	F	≥90		6.0
KYS05090S[e]		H	H	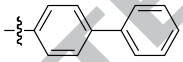	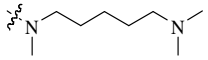	H	≥90	3.6	6.0

[a] Values represent the mean of three independent experiments; [b] $Ca_v3.2$ (α_{1H}); [c] Whole-cell patch clamp recording in HEK cells; [d] Non-small cell lung cancer cells; [e] Dihydrochloride salt was used as a parent compound.

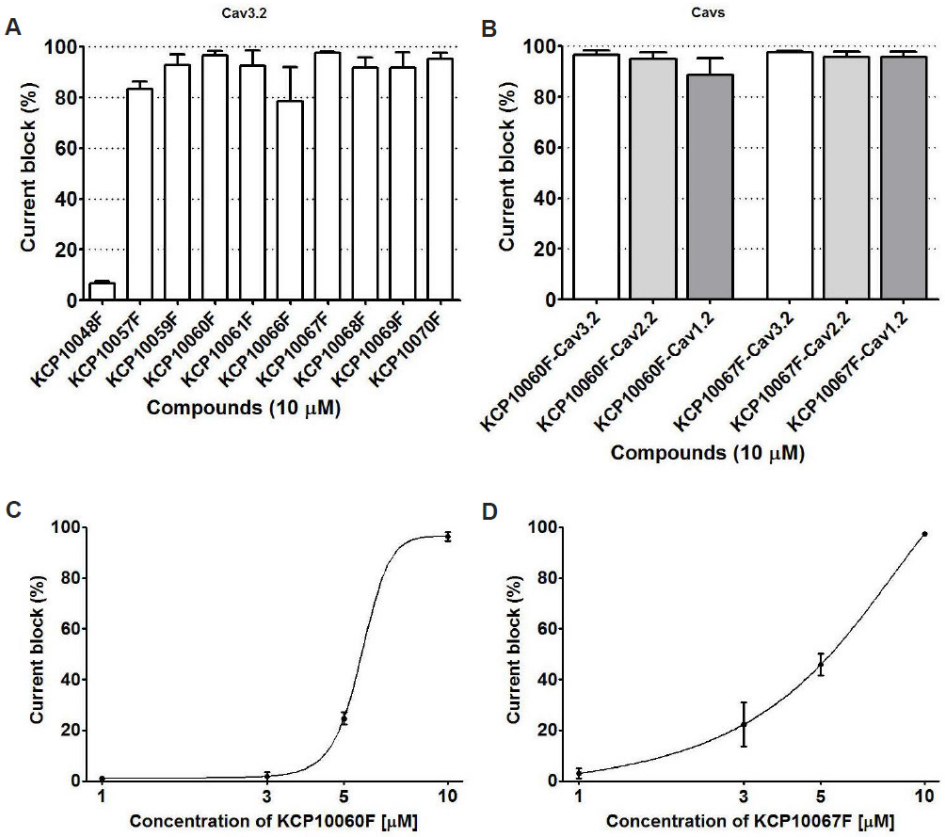

Figure 2. (**A**) Percentage of whole cell current inhibition of $Ca_v3.2$ (T-type) in response to 10 μM application of the compound series (n = 3 per compound); (**B**) Percentage of whole cell current inhibition of $Ca_v3.2$ (T-type), $Ca_v2.2$ (N-type), and $Ca_v1.2$ (L-type) in response to 10 μM application of compound **8d** (KCP10060F – three bars at the left side) and **8g** (KCP10067F – three bars at the right side) (n = 3 per channel); (**C**) Dose-response relation for **8d** (KCP10060F); (**D**) Dose-response relation for **8g** (KCP10067F) block of $Ca_v3.2$ (T-type). The IC_{50} values from the fitted curve were 5.61±1.81 and 5.11±1.32 μM (n = 3 per dose), respectively. The hill coefficients for compounds **8d** and **8g** were 0.8 and 0.14, respectively.

Current–voltage relationship experiments for both compounds were carried out for $Ca_v3.2$ channels transiently transfected into HEK-293 cells by stepping to a series of test potentials ranging from −60 mV to +60 mV in 10 mV steps (lasting for 100 ms). Fig. 3A and 3B display averaged IV-traces from cells before and after the application of 5 μM **8d** (KCP10060F) and **8g** (KCP10067F), respectively. Each compound caused a prominent reduction of peak current density compared to the control across a range of test potentials. However, neither compound **8d** (KCP10060F) nor **8g** (KCP10067F) caused a shift in the half-activation potential.

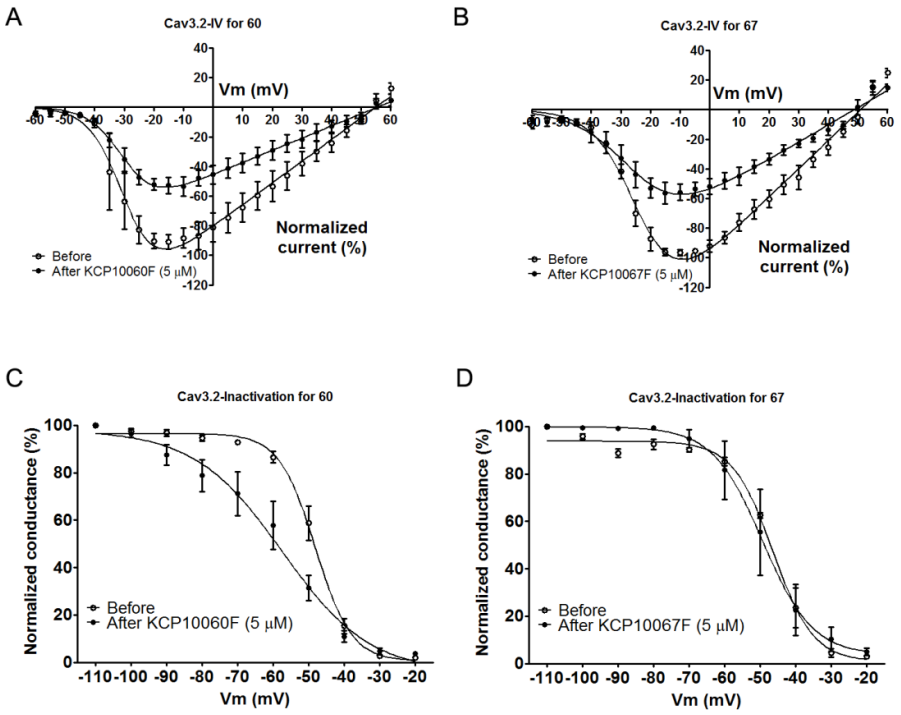

Figure 3. (**A**) and (**B**): Effects of **8d** (KCP10060F) and **8g** (KCP10067F) on the current-voltage relation of $Ca_v3.2$ (T-type), respectively. The half activation potential ($Va_{1/2}$) from the fitted curves was not affected by the blockers (-29.82±1.12 mV and -29.94±1.06 mV before after the application of **8d** (KCP10060F, 5 µM, n = 3), (p = 0.90, paired t-test); -23.49±0.75 mV and -24.71±1.61 mV before and after the application of **8g** (KCP10067F, 5 µM, n = 3), (p = 0.27, paired t-test); (**C**) and (**D**): Effects of **8d** (KCP10060F) and **8g** (KCP10067F) on the steady-state inactivation curve of $Ca_v3.2$ (T-type), respectively. The half inactivation potential from the fitted curves was shifted from -48.12±0.62 mV to -57.43±2.76 mV after the application of **8d** (KCP10060F, 5 µM, n = 6), (p = 0.03, paired t-test), whereas there was no effect of **8g** (-46.36±0.85 mV and -49.29±2.18 mV before and after the application of **8g** (KCP10067F, 5 µM, n = 3), (p = 0.38, paired t-test), respectively.

A two-step voltage-clamp protocol was applied for determining the effects of the compounds on steady-state inactivation of $Ca_v3.2$. This involved an inactivating pre-pulse period that varied from −110 mV to -20 mV. The test current amplitude at each pulse potential was normalized to the maximal amplitude of this current (I/I_{max}). Data were fitted to the Boltzmann equation. As shown in Fig. 3C and 3D, 5 µM of **8d** (KCP10060F) but not **8g** (KCP10067F) shifted the voltage-dependence of the inactivation toward more negative potentials (from -48.12±0.62 mV to -57.43±2.76 mV for **8d**). This suggests that **8d** interacts with the inactivated state of the channel, suggesting that this compound will show an enhanced blocking affect at typical neuronal resting

potentials and may display use-dependent properties.

All derivatives were evaluated for anti-proliferative activity against A549 (non-small cell lung cancer cells) using MTT assay.[36] The overall biological results for the inhibition of calcium influx and the cytotoxicity on human cancer cells were summarized in Table 2 together with those of KYS05090S as a positive control. The compounds exhibited different degrees of cytotoxic activity (IC_{50} = <10 μM) in A549 cell lines, with some being more potent than KYS05090S. Interestingly, compound **8a** (KYS10048F) was as active as KYS05090S irrespective of its lower T-type channel blocking effect. Compound **8c** (KCP10059F) containing a 4-fluorobiphenylyl ring at R^4 and fluorine atom at R^5 was most active (IC_{50} = 2.2 μM) and 3-fold more active than KYS05090S (IC_{50} = 6.0 μM). Compound **8d** (KCP10060F) and **8g** (KCP10067F) had an IC_{50} of 5.1 and 7.6 μM, respectively, against A549 cell lines.

We also explored the in vitro metabolic stability of selected compounds in rat and human liver microsomes using a single point metabolic assay.[37] Among them, 5 compounds (**8c**-**8e**, **8h** and **8j**) and 3 compounds (**8e**, **8h** and **8j**) exhibited improved liver metabolic stability in rat (48-76% remaining after 30 min incubation) and human (42-54% remaining after 30 min incubation), respectively, compared to KYS05090S. It can be assumed that a fluorine atom (that is, R^5 substituent) at the *para*-position of the benzyl amide and a 4-cyclohexylphenyl ring instead of the biphenyl ring as the R^3 substituent are the main factors contributing to the metabolic stability. A possible explanation is these two structural changes can block the *para*-hydroxylation which can occur to both the phenyl ring of benzyl amide group and the phenyl ring of the biphenyl group. Among the tested compounds, therefore, **8h** (KCP10068F) containing both 4-fluorobenzyl amide and 4-cyclohexylphenyl ring showed the best metabolic stability, which is approximately a 2-fold increase in liver metabolic stability in two species compared to KYS05090S as shown in Table 3.

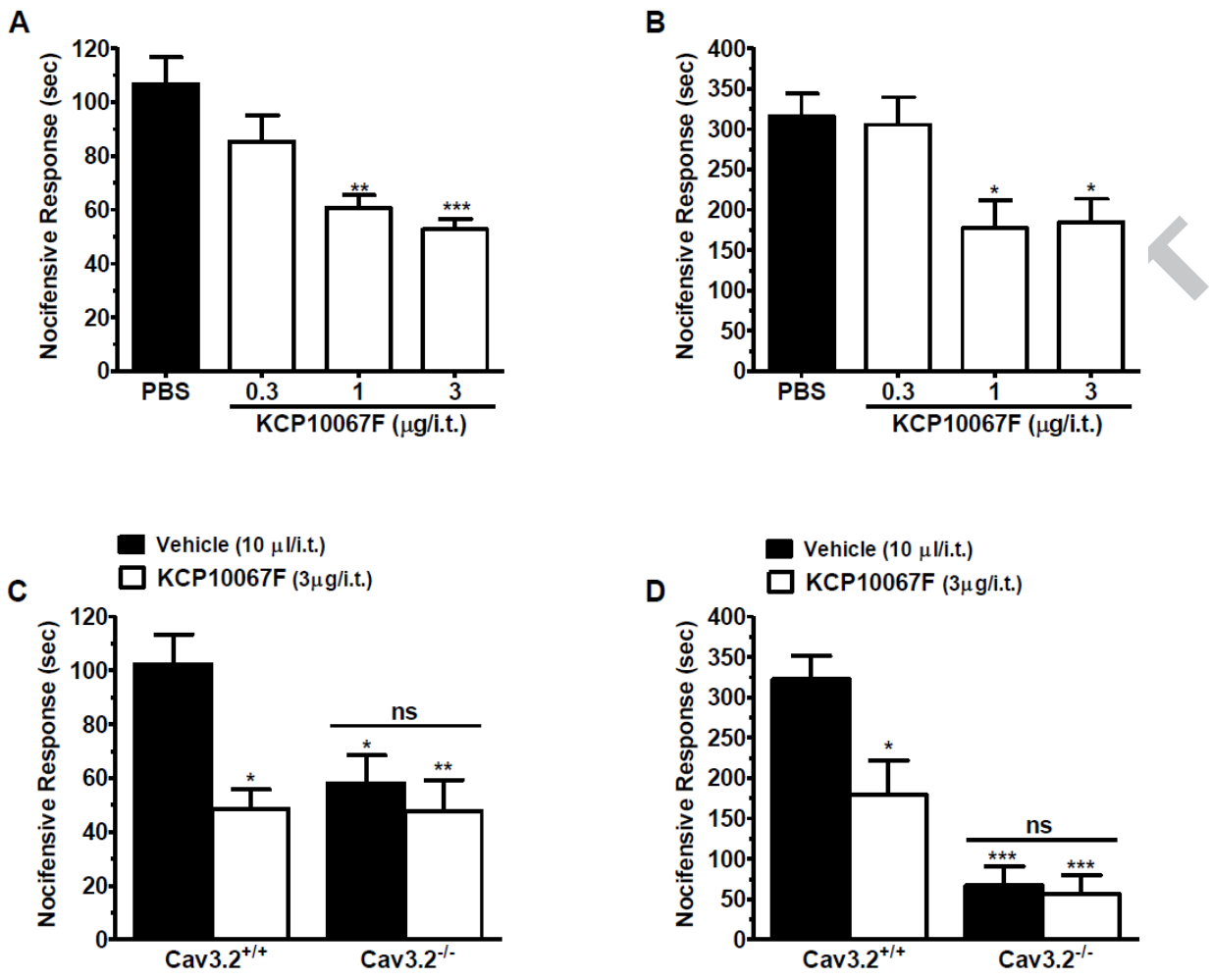

Figure 4. (**A**) and (**B**): Dose-dependent effect of intrathecally delivered **8g** (KCP10067F) on the first and second phases of formalin-induced pain in mice (n = 7-9), respectively; (**C**) and (**D**): Effect of **8g** delivered intrathecally to $Ca_v3.2$ null mice in the first and second phases of the formalin test (n = 6-7), respectively. Each bar represents the mean±SEM and is representative of 2 independent experiments. Asterisks denote the significance relative to the control group (A, B) or yet to the wild type group treated with vehicle (C, D) (*p < 0.05, **p < 0.01, ***p < 0.001, one-way ANOVA followed by Tukey's test).

$Ca_v3.2$ calcium channels are also a potential target for pain therapeutics. The ability of **8g** (KCP10067F) to inhibit inflammatory pain responses was thus also examined, using approaches that have been described by us in detail previously.[38-40] The formalin test involves the injection of formalin into the hindpaw, which triggers two distinct phases of nocifensive behavior (i.e., biting and licking of the paw), whose durations can be determined in the absence and the presence of the compounds. Increasing doses of compound **8g** mediated analgesic effects in both nocifensive

phases in the formalin test (Fig. 4A and 4B), as evident from a shortening of the nocifensive response duration. This effect was ablated in mice lacking $Ca_v3.2$ channels (Fig. 4C and 4D), indicating that the physiological effects of compound **8g** were mediated by action on $Ca_v3.2$, rather than on another target such as $Ca_v2.2$ or $Ca_v1.2$. Compound **8g** (KCP10067F) was also partially effective in reversing mechanical hypersensitivity in mice subjected to intraplantar injection of complete Freund's Adjuvant (CFA) (Fig. 5), where a small **8g**-induced increase in mechanical paw withdrawal was observed. Altogether, these data indicate that compound **8g** partially protects from inflammatory hypersensitivity.

Table 3. *In vitro* liver microsomal stability of selected compounds [a]

Entry	Code (KCP)	%remaining after 30 min incubation	
		Rat	Human
8c	**10059F**	64.5	29.2
8d	**10060F**	47.9	20.1
8e	**10061F**	65.7	42.1
8g	**10067F**	22.3	20.3
8h	**10068F**	70.1	54.0
8j	**10070F**	75.8	44.2
KYS05090S		37.8	27.3
Verapamil [b]			9.0

[a] The metabolic stability was expressed as percent remaining compound after 30 minutes incubation in liver microsomal enzyme; [b] Reference compound.

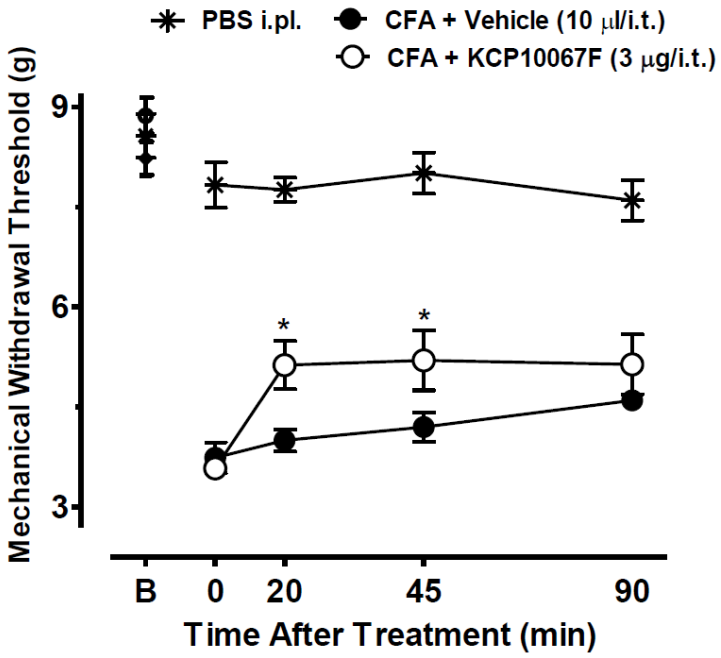

Figure 5. Blind analysis of the time course of mechanical hyperalgesia of CFA-injected mice treated with either vehicle or **8g** (KCP10067F). Each circle represents the mean ± SEM (n = 8-11), and is representative of 2 independent batches of mice. (*$p < 0.05$, ***$p < 0.001$, two-way ANOVA followed by Tukey's test). Animals injected with CFA significantly differed from the sham treated group ($p < 0.001$).

3. Conclusions

In this study, the introduction of fluorine atom into lead compound KYS05090S via a bioisosteric strategy led to a series of fluoro-substituted 3,4-dihydroquinazoline derivatives, which were evaluated for T-type Ca^{2+} channel blocking ability and in vitro cytotoxic activity against A-549 cells. Most of the novel 3,4-dihydroquinazoline derivatives displayed good T-type Ca^{2+} channel blocking effects (≥90% inhibition at 10 μM), along with potent inhibition of L-type and N-type channels, and cytotoxic activity (IC_{50} = <9 μM), especially compound **8h** (KCP10068F) which exhibited particularly good cytotoxic activity (IC_{50} = 5.9 μM) comparable to the reference compound KYS05090S with improved human and rat liver microsomal stability. Thus, compound **8h** (KCP10068F) may represent a good backup compound for KYS05090S for further biological investigations as cytotoxic agents. In addition, compound **8g** (KCP10067F) was found to partially protect from inflammatory pain via the blockade of $Ca_v3.2$ channel.

4. Experimental section

4.1. Chemistry

4.1.1. General

All solvents and commercially available reagents were used without additional purification. Reactions were monitored by analytical thin layer chromatography (TLC, Merck, silica gel 60 F_{254}) with UV light (254 nm). Visualization was performed by incubation with *p*-methoxyanisaldehyde (PMA) solution and heating with a heat gun. Flash column chromatography was performed using a silica gel (Merck, 230–400 mesh). Melting points were recorded on electrothermal MEL-TEMP® 3.0 capillary melting point apparatus and are uncorrected. NMR spectra (^{1}H and ^{13}C) were recorded on Bruker Avance 400 MHz spectrometers. High-resolution mass spectra (ESI, positive/negative ion mode) were obtained using SYNAPT G2-Si mass spectrometry, Waters.

4.1.2. Synthesis of compounds except **8f** (KCP10066f) listed in Table 2 were previously reported by our group.[20, 33]

4.1.3. Preparation of compound 2: To a solution of methyl *trans*-2-nitrocinnamate (**1**, 3.76 g, 18.14 mmol) in MeOH (100 mL) was added activated Zn powder (8.04 g, 145.16 mmol) and NH_4Cl (2.14 g, 39.32 mmol) at 0℃ and the solution was heated at reflux for 12 h. The resulting mixture was filtered through celite 545 and evaporated *in vacuo* to give the crude product. The concentrated product was poured into EtOAc (100 mL) and stayed under sonicator for 10 min. EtOAc-insoluble matter was filtered off and the filtrate was washed with sat. $NaHCO_3$, dried ($MgSO_4$), evaporated *in vacuo* to give the desired product **2** (3.16 g, 98%) as an orange color solid: mp 61.1-62.2 ℃; ^{1}H NMR (400 MHz, $CDCl_3$) δ 7.83 (1H, d, *J* = 15.6 Hz), 7.38 (1H, dd, *J* = 8 and 1.6 Hz), 7.19 (1H, t, *J* = 8 Hz), 6.77 (1H, t, *J* = 7.6 Hz), 6.72 (1H, dd, *J* = 8 and 0.8 Hz), 6.35 (1H, d, *J* = 16.0 Hz), 3.97 (2H, br s), 3.80 (3H, s); ^{13}C NMR (100 MHz, $CDCl_3$) δ 167.7, 145.5, 140.3, 131.3, 128.1, 119.9, 119.0, 117.7, 116.8, 51.7; HRMS (ESI+): calcd for $C_{10}H_{12}NO_2$ (M+H) 178.0868, found: 178.0866.

4.1.4. Preparation of compound 4: To a solution of 4-(4-fluorophenyl)benzoic acid (**3**, 0.65 g, 3.01 mmol) in distilled toluene (20 mL) was added 97% diphenylphosphonic azide (DPPA) (0.78 mL, 3.61 mmol) and Et_3N (0.89 mL, 6.01 mmol) at rt for Curtius rearrangement. The reaction mixture was stirred at rt for 3 h, further stirred at 100 ℃ for 6 h, followed by an addition of a solution of methyl 2-aminocinnamate (**2**, 0.53 g, 3.01 mmol) in distilled toluene (20 mL) at rt. The reaction mixture was stirred at rt overnight and concentrated under reduced pressure to give a solid, which was washed with MeOH (50 mL) to give the desired product **4** (0.63 g, 54%) as a white solid: mp 218.3-222.7 ℃; ^{1}H NMR (400 MHz, DMSO) δ 9.09 (1H, s), 8.57 (1H, s), 7.90 (1H, d, *J* = 15.6 Hz),

7.78 (2H, dd, *J* = 8.0 and 3.6 Hz), 7.68 (2H, dd, *J* = 8.8 and 6.0 Hz), 7.58 (4H, dd, *J* = 15.6 and 8.8 Hz), 7.43-7.39 (1H, m), 7.27 (2H, t, *J* = 8.8 Hz), 7.15 (1H, t, *J* = 7.6 Hz), 6.61 (1H, d, *J* = 15.6 Hz), 3.75 (3H, s); ^{13}C NMR (100 MHz, DMSO) δ 166.7, 162.7, 160.3, 152.7, 139.8, 139.1, 137.8, 136.3, 132.6, 130.7, 128.0, 127.9, 127.1, 127.0, 126.1, 123.9, 123.7, 118.8, 118.5, 115.7, 115.5, 51.5; HRMS (ESI+): m/z calcd. for $C_{23}H_{19}FN_2NaO_3$ $[M+Na]^+$ 413.1277, found 413.1272.

4.1.5. Preparation of compound 5: A solution of urea (**4**, 0.63 g,1.61 mmol) in distilled CH_2Cl_2 (20 mL) and Et_3N (0.67 mL, 4.84 mmol) was added into a solution of dibromotriphenylphosphorane (1.02 g, 2.42 mmol) in distilled CH_2Cl_2 (10 mL) at 0℃ under Ar. The reaction mixture was stirred at the same temperature for 12 h and treated with water (30 mL). The mixture was extracted with CH_2Cl_2 (3×), dried ($MgSO_4$), and concentrated under reduced pressure. The residue was briefly purified by flash column chromatography (EtOAc:Hexane = 1:20) to provide the desired product **5** (0.23 g, 38%) as a yellow oil, which was used for next reaction without further purification: ^{1}H NMR (400 MHz, DMSO) δ 8.03 (1H, d, *J* = 16.0 Hz), 7.89 (1H, d, *J* = 16.0 Hz), 7.74-7.68 (4H, m), 7.49-7.43 (2H, m), 7.37 (2H, d, *J* = 16.0 Hz), 7.32-7.28 (3H, m), 6.72 (1H, d, *J* = 16.0 Hz), 3.74 (3H, s);

4.1.6. General of compound 7: To a solution of carbodiimide compound (**5**, 0.51 g, 1.38 mmol) in MeOH (30 mL) was added a solution of 1-[2-(1-pyrrolidinyl)ethyl]piperazine (**6**, 0.22 g, 1.18 mmol) in MeOH (5 mL) and the mixture solution was stirred for 4 h. The mixture was concentrated *in vacuo* and subjected to flash column chromatography (CH_2Cl_2:MeOH:NH_4OH = 100:9:1) to provide the desired product (**7**, 0.46 g, 69%) as a white solid: mp 61.0-64.2 ℃; ^{1}H NMR (400 MHz, $CDCl_3$) δ 7.50-7.46 (2H, m), 7.43-7.41 (2H, m), 7.26-7.19 (2H, m), 7.16-7.08 (4H, m), 7.00-6.93 (2H, m), 5.15 (1H, dd, *J* = 10.8 and 4.8 Hz), 3.77 (3H, s), 3.49 (4H, br s), 2.86 (1H, dd, *J* = 15.2 and 10.8 Hz), 2.64-2.60 (2H, m), 2.57-2.51 (7H, m), 2.40 (4H, br s), 1.78 (6H, s); ^{13}C NMR (100 MHz, $CDCl_3$) δ 171.9, 163.6, 161.1, 152.4, 144.9, 143.7, 136.4, 135.8, 128.5, 128.4, 128.3, 127.7, 125.8, 124.7, 123.0, 122.6, 122.3, 115.8, 115.5, 60.9, 57.6, 54.6, 53.7, 53.2, 51.9, 45.6, 39.5, 23.4; HRMS (ESI+): m/z calcd. for $C_{33}H_{39}FN_5O_2$ $[M+H]^+$ 556.3088, found 556.3084.

4.1.7. Preparation of compound 8f (KCP10066F): The reaction mixture containing ester **7** (0.46 g, 0.82 mmol), 1,5,7-triazabicyclo[4,4,0]dec-5-ene (TBD: 0.034 g, 0.25 mmol) as a catalyst, and 4-fluorobenzylamine (0.25 g, 1.97 mmol) was stirred at 40 ℃ for 12 h under solvent-free condition. Flash column chromatography (CH_2Cl_2:MeOH:NH_4OH = 100:14:1) of the resultant mixture gave the desired product (**8f**, 0.46 g, 87%) as a pale yellow solid: mp 85.2-95.4 ℃; ^{1}H NMR (400 MHz, $CDCl_3$) δ 7.79 (1H, s), 7.45 (2H, dd, *J* = 8.0 and 5.2 Hz), 7.38 (2H, d, *J* = 8.4 Hz), 7.28 (2H, dd, *J* = 8.0 and 5.6 Hz), 7.17 (2H, d, *J* = 8.4 Hz), 7.12 (1H, d, *J* = 7.2 Hz), 7.07 (2H, t, *J* = 8.8 Hz), 7.00 (1H, d, *J* = 7.6 Hz), 6.91 (4H, m), 5.24 (1H, dd, *J* = 8.8 and 4.8 Hz), 4.46 (2H, m), 3.20 (4H, s), 2.63 (4H,

s), 2.56 (3H, m), 2.44 (2H, d, *J* = 5.6 Hz), 2.31 (1H, dd, *J* = 14.4 and 5.2 Hz), 2.11 (4H, s), 1.80 (4H, s); ^{13}C-NMR (100 MHz, $CDCl_3$) δ 169.4, 162.7, 162.4, 160.2, 159.9, 152.4, 144.0, 142.2, 135.6, 135.5, 135.1, 134.1, 134.0, 129.3, 129.2, 127.6, 127.5, 126.8, 125.9, 124.3, 122.1, 122.0, 121.3, 114.9, 114.7, 114.6, 114.4, 59.9, 55.7, 53.7, 52.5, 51.8, 45.1, 41.9, 40.6, 22.5; HRMS (ESI+): m/z calcd. for $C_{39}H_{43}F_2N_6O$ $[M+H]^+$ 649.3466, found 649.3464.

4.2. Biological evaluation

4.2.1. Cell culture for MTT assay

Human lung adenocarcinoma A549 cells were obtained from the Korean cell line bank (Seoul, Korea). Cells were cultured in RPMI 1640 supplemented with 10% heat-inactivated FBS, penicillin (100 U/mL) and streptomycin sulfate (100 μg/mL). Cells were cultured at 37 °C in an atmosphere of 5% CO_2.

4.2.2. MTT assay

The cells (5×10^4/mL) were seeded in each well containing 100 μL of the RPMI medium supplemented with 10% FBS in a 96-well plate. Various concentrations of synthetic compound were added and incubated for 24 h. MTT (5 mg/mL stock solution) was added and the plates were incubated for an additional 4 h. The medium was discarded and the formazan blue, which was formed in the cells, was dissolved with 100 μL DMSO. The optical density was measured at 540 nm by an automatic microplate reader (Molecular Devices Corp., Sunnyvale, CA, USA).

4.2.3. Cell culture and transient transfection for electrophysiology

HEK tsA-201 cells were grown to 80～90% confluence at 37 °C (5 % CO_2) in DMEM medium (Life Technologies, Grand Island, NY, USA), supplemented with 10 % (vol/vol) FBS (HyClone, Thermo Scientific, Pittsburgh, PA, USA), 200 U/ml penicillin, and 0.2 mg/ml streptomycin (Life Technologies). Cells were suspended with 0.25% trypsin/EDTA and plated onto glass coverslips in 10-cm culture dishes (Corning, Corning, NY, USA) at 10% confluence 24 h before transfection. Calcium channel (6 μg) and GFP marker (0.6 μg) DNAs were transfected into cells with calcium phosphate. For $Ca_v2.2$ and $Ca_v1.2$ channels, cDNA encoding $Ca_v\alpha2\delta1$ and $Ca_v\beta1b$ subunits were co-transfected. Cells were transferred to 30 °C 16–18 h later following transfection and stored for 2 days before recording.

4.2.4. Electrophysiology

Cells on a glass coverslip were transferred into an external bath solution of 20 mM $BaCl_2$, 1 mM $MgCl_2$, 40 mM TEACl, 65 mM CsCl, 10 mM HEPES, 10 mM glucose, pH 7.4. Borosilicate

glass pipettes (Sutter Instrument Co., Novato, CA, USA) (3–5 MΩ) were filled with internal solution containing 140 mM CsCl, 2.5 mM $CaCl_2$, 1 mM $MgCl_2$, 5 mM EGTA, 10 mM HEPES, 2 mM Na-ATP, and 0.3 mM Na-GTP, pH 7.3. Whole-cell patch clamp recordings were performed by using an EPC 10 amplifier (HEKA Elektronik, Bellmore, NY, USA) linked to a personal computer equipped with Pulse (V8.65) software (HEKA Elektronik). After seal formation, the membrane beneath the pipette was ruptured and the pipette solution was allowed to dialyze into the cell for 2–5 min before recording. T-type calcium currents were elicited by depolarization from a holding potential of −110 mV to a test potential of −20 mV for 100 ms with an interpulse interval of 20 s. Voltage-dependent currents were leak corrected with an online P/4 subtraction paradigm. Data were recorded at 10 kHz and filtered at 2.9 kHz. Data analysis was performed by using online analysis built in Pulse software, and graphs were prepared by using GraphPad Prism 5 (GraphPad Software, La Jolla, CA, USA). Error bars plotted represent the mean values±standard error.

4.2.5. Animals

Experiments were carried out using either adult male C57BL/6J (wild-type) or CACNA1H knockout ($Ca_v3.2$ null) mice (20–25g) purchased from Jackson Laboratories. Animals were used at a maximum of five mice per cage (30×20×15 cm^3) with free access to food and water and temperature kept at 23±1 °C on a 12 h light/dark cycle (lights on at 7:00 a.m.). Best efforts were made to minimize animal suffering and distress according to the policies and recommendations of the International Association for the Study of Pain and the guidelines of the Canadian Council on Animal Care, all protocols were approved by the Institutional Animal Care and Use Committee. Intrathecal (i.t.) injections were given using volumes of 10 μL and performed according to the method described by Hylden and Wilcox[41] and carried out routinely in our laboratory.[39] All drugs were dissolved in 2% or less DMSO, whereas control animals received PBS + 2% DMSO. For each test, a different group of mice were used and only one experiment per mouse was performed. The experimenter was blinded to the experimental groups when testing the action of **8g** (KCP10067F) on CFA-injected animals.

4.2.6. Formalin Test

Animals were left to acclimatize for at least 60 min before the experiments. They were injected intraplantarily (i.pl.) in the ventral surface of the right hind paw with 20 μL of a formalin solution (1.25%) made up in PBS. Immediately after formalin injection, mice were individually placed into observation chambers and tested from 0 to 5 min (acute nociceptive phase) and 15–30 min (inflammatory phase). Time spent licking or biting the injected paw was considered as a nocifensive response and recorded with a chronometer. Different doses of **8g** (KCP10067F) (0.3 – 3 μg/i.t.) were delivered intrathecally 20 min prior to formalin and the effects of treatments were

analyzed.

4.2.7. Persistent inflammatory pain induced by CFA

In order to induce mechanical hyperalgesia in mice triggered by peripheral inflammation, 20 µL of Complete Freund's Adjuvant (CFA) was injected subcutaneously in the plantar surface of the right hindpaw (i.pl.) and animals in the sham group received 20 µl of PBS in the ipsilateral paw accordingly to the method previously reported by Ferreira et al.[42] Animals were treated with either vehicle (10 µL/i.t.) or **8g** (KCP10067F) (3 µg/i.t.) 2 days following CFA injections and their mechanical withdrawal thresholds were analyzed time-dependently.

4.2.8. Evaluation of Mechanical Hyperalgesia

Mechanical hyperalgesia measurements were taken before injection of CFA and 2 daysafter CFA and prior to **8g** (KCP10067F) delivery (0), and also at different time points (20, 45, 90 min) after treatment. Measurements were taken using a Dynamic Plantar Aesthesiometer (DPA, Ugo Basile, Varese, Italy). Mice were individually placed in small enclosed transparent testing chambers (20 × 18.5 × 13 cm^3, length × width × height) on top of a grid floor and allowed to acclimate for a period of at least 90 min. The DPA device was then positioned underneath so thatthe filament was directly below the plantar surface of the ipsilateral hind paw of the animal and tested three times per time point.

4.2.9. Statistical analysis

For behavioral experiments, data are presented as mean±SEM and analyzed by either one-way or two-way analysis of variance (ANOVA) followed by Tukey's test. A value of $p < 0.05$ was considered to be significant (*p <0.05; **p <0.01; ***p <0.001; NS = not different).

4.2.10. Microsomal stability

The microsomal clearance of the test compounds was evaluated using a single point metabolic assay. Incubation mixtures contained 0.5 mg/mL human liver microsomes or 0.5 mg/mL rat liver microsomes, 1 µM compound in 0.1 M phosphate buffer (pH 7.4) at 37 °C for 5 min. The reaction was started by adding NADPH regeneration system solution and was incubated at 37 °C for 30min. Acetonitrile solution containing chlorpropamide as an internal standard was added to stop the reaction. The sample was centrifuged (14,000 rpm, 4 °C) for 5 min. The supernatant was run on a Shimadzu Nexera XR system and TSQ vantage (Thermo). A Kinetex C_{18} column (50 × 2.1 mm, 2.6 µm particle size, Phenomenex) was used for the analysis. The mobile phase used was 0.1% formic acid in water (A) and 0.1% formic acid in acetonitrile (B). Data were processed on Analyst software (version 1.6.1) and Xcalibur (version 1.6.1).

Acknowledgments

This work was supported by Basic Science Research Program through the Ministry of Education of the Republic of Korea and the National Research Foundation (NRF-2016R1D1A1B03936197), and the Canadian Institutes of Health Research and Canada Research Chair Program (GWZ).

References and Notes

1. Berridge, M. J.; Lipp, P.; Bootman, M. D. *Nat. Rev. Mol. Cell Biol.* **2000**, *1*, 11.
2. Berridge, M. J.; Bootman, M. D.; Roderick, H. L. *Nat. Rev. Mol. Cell Biol.* **2003**, *4*, 517.
3. Clapham, D. E. *Cell*, **2007**, *131*, 1047.
4. Parkash, J.; Asotra, K. *Life Sci*. **2010**, *87*, 587.
5. Akl, H.; Bultynck, G. *Biochim. Biophys. Acta*. **2013**, *1835*, 180.
6. Stewart, T. A.; Yapa, K.T.; Monteith, G. R. *Biochim. Biophys. Acta*. **2015**, *1848*, 2502.
7. Chen, Y. F.; Chen, Y. T.; Chiu, W. T.; Shen, M. R. *J. Biomed. Sci*. **2013**, *20*, 23.
8. Taylor, J. T.; Zeng, X. B.; Pottle, J. E.; Lee, K.; Wang, A. R.; Yi, S. G.; Scruggs, J. A.; Sikka, S. S.; Li M. World J. Gastroenterol. **2008**, *14*, 4984.
9. Lory, P.; Bidaud, I.; Chemin, J. *Cell Calcium* **2006**, *40*, 135.
10. Gray, L. S.; Perez-Reyes, E.; Gamorra, J. C.; Haverstick, D. M.; Shattock, M.; McLatchie, L.; Harper, J.; Brooks, G.; Heady, T.; Macdonald, T. L. *Cell Calcium* **2004**, *36*, 489.
11. Yunker, A. M.; McEnery, M. W. *J. Bioenerg. Biomembr.* **2003**, *35*, 533.
12. Monteil, A.; Chemin, J.; Leuranguer, V.; Altier, C.; Mennessier, G.; Bourinet, E.; Lory, P.; Nargeot, J. *J. Biol. Chem*. **2000**, *275*, 16530.
13. Chemin, J.; Monteil, A.; Lory, P. *J. Soc. Biol*. **2003**, *197*, 235.
14. Berridge, M. J. *Neuron* **1988**, *21*, 13.
15. Perez-Reyes, E.; Lory, P. *CNS Neurol. Disord.: Drug Targets* **2006**, *5*, 605.
16. Lastraioli, E.; Iorio, J.; Arcangeli, A. *Biochim. Biophys. Acta*. **2015**, *1848*, 2685.
17. Nilius, B.; Carbone, E. *Pflügers Arch.* **2014**, *466*, 689.
18. Dziegielewska, B.; Gray, L. S.; Dziegielewski, J. *Pflügers Arch.* **2014**, *466*, 801.

19. Santoni, G.; Santoni, M.; Nabissi, M. *Br. J. Pharmacol*. **2012**, *166*, 1244.

20. Byun, J. S.; Sohn, J. M.; Leem, D. G.; Park, B.; Nam, J. H.; Shin, D. H.; Shin, J. S.; Kim, J. H.; Lee, K.-T.; Lee, J. Y. *Bioorg. Med. Chem. Lett*. **2016**, 26, 1073.

21. Rim, H. K.; Cho, S.; Shin, D. H.; Chung, K. S.; Cho, Y. W.; Choi, J. H.; Lee, J. Y.; Lee, K.-T. *Molecules* **2014**, *19*, 9864.

22. Choi, D. L.; Jang, S. J.; Cho, S.; Choi, H. E.; Rim, H. K.; Lee, K.-T.; Lee, J. Y. *Bioorg. Med. Chem. Lett.* **2014**, *24*, 1565.

23. Jang, S. J.; Choi, H. W.; Choi, D. L.; Cho, S.; Rim, H. K.; Choi, H. E.; Kim, K. S.; Huang, M.; Rhim, H.; Lee, K.-T.; Lee, J. Y. *Bioorg. Med. Chem. Lett.* **2013**, *23*, 6656.

24. Rim, H. K.; Lee, H. W.; Choi, I. S.; Park, J. Y.; Choi, H. W.; Choi, J. H.; Cho, Y. W.; Lee, J. Y.; Lee, K.-T. *Bioorg. Med. Chem. Lett*. **2012**, *22*, 7123.

25. Kang, H. B.; Rim, H. K.; Park, J. Y.; Choi, H. W.; Choi, D. L.; Seo, J. H.; Chung, K. S.; Huh, G.; Kim, J.; Choo, D. J.; Lee, K.-T.; Lee, J. Y. *Bioorg. Med. Chem. Lett*. **2012**, *22*, 1198.

26. Seo, H. N.; Choi, J. Y.; Choe, Y. J.; Kim, Y.; Rhim, H.; Lee, S. H.; Kim, J.; Joo, D. J.; Lee, J. Y. *Bioorg. Med. Chem. Lett*. **2007**, *17*, 5740.

27. Choi, T. A.; Furimsky, A. M.; Swezey, R.; Bunin, D. I.; Byrge, P.; Iyer, L. V.; Chang, P. Y.; Abergel, R. J. *J. Pharm. Sci*. **2015**, 104, 1832

28. Di, L.; Kerns, E. H.; Gao, N.; Li, S. Q.; Huang, Y.; Bourassa, J. L.; Huryn, D. M. *J. Pharm. Sci*. **2004**, *93*, 1537.

29. Böhm, H. J.; Banner, D.; Bendels, S.; Kansy, M.; Kuhn, B.; Müller, K.; Obst-Sander, U.; Stahl, M. *ChemBioChem.* **2004**, *5*, 637.

30. Shah, P.; Westwell, A. D. *J. Enzyme Inhib. Med. Chem.* **2007**, *22*, 527.

31. Müller, K.; Faeh, C.; Diederich, F. *Science* **2007**, *317*, 1881.

32. Littke, A. F.; Fu, G. C. *Org. Synth*. **2005**, *81*, 63.

33. Park, B.; Nam, J. H.; Kim, J H.; Kim, H. J.; Onnis, V.; Balboni, G.; Lee, K.-T.; Park, J. H.; Catto, M.; Carotti, A.; Lee, J. Y. Bioorg. Med. Chem. Lett. **2017**, *27*, 1179.

34. M'Dahoma, S.; Gadotti, V. M.; Zhang, F. X.; Park, B.; Nam, J. H.; Onnis, V.; Balboni, G.; Lee, J. Y.; Zamponi, G. W. *Pflügers Arch*. **2016**, *468*, 193.

35. Park, S. J.; Park, S. J.; Lee, M. J.; Rhim, H.; Kim, Y.; Lee, J. H.; Chung, B. Y.; Lee, J. Y. *Bioorg. Med. Chem.* **2006**, *14*, 3502.

36. Rubinstein, L. V.; Shoemaker RH.; Paull KD.; Simon RM.; Tosini S;; Skehan P.; Scudiero DA.; Monks A.; Boyd, M. R. *J. Natl. Cancer Inst*. **1990**, *82*, 1113.

37. Di, L.; Kerns, E. H.; Gao, N.; Li, S. Q.; Huang; Y.; Bourassa, J. L.; Huryn, D. M. *J. Pharm. Sci*. **2004**, *93*,1537.

38. Gadotti, V. M.; You, H.; Petrov, R. R.; Berger, N. D.; Diaz, P.; Zamponi, G. W. *Mol. Pain* **2013**, *9*, 32.

39. Bladen, C.; McDaniel, S. W.; Gadotti, V. M.; Petrov, R. R.; Berger, N. D.; Diaz, P.; Zamponi, G. W. *ACS Chem. Neurosci*. **2015**, *6*, 277.

40. Gadotti, V. M.; Caballero, A. G.; Berger, N. D.; Gladding, C. M.; Chen, L.; Pfeifer, T. A.; Zamponi, G. W. *Mol. Pain* **2015**, *11*, 12.

41. Hylden, J. L.; Wilcox, G. L. *Eur. J. Pharmacol.* **1980**,*67,* 313.

42. Ferreira, J.; Campos, M. M.; Pesquero, J. B.; Araujo, R. C.; Bader, M.; Calixto, J. B. *Neuropharmacology*. **2001**, *41*, 1006.

Graphical Abstract

Synthesis and biological evaluation of fluoro-substituted 3,4-dihydroquinazoline derivatives for cytotoxic and analgesic effects

Jin Han Kim, Hui Rak Jeong, Da Woon Jung, Hong Bin Yoon, Sun Young Kim, Hyoung Ja Kim, Kyung-Tae Lee*, Vinicius M. Gadotti, Junting Huang, Fang-Xiong Zhang, Gerald W. Zamponi*, Jae Yeol Lee*

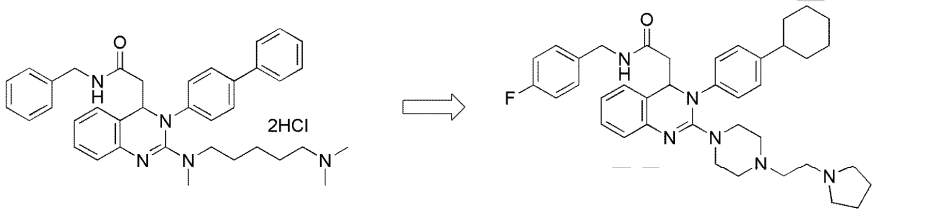

KYS05090S

T-Type Ca^{2+} channel: >90% inhibition at 10 μM
A549 cancer cells; IC_{50} = 6.0 μM
Liver microsomal stablity: 27.3% (human), 37.8% (rat)

8h (KCP10068F)

T-Type Ca^{2+} channel: >90% inhibition at 10 μM
A549 cancer cells; IC_{50} = 5.9 μM
Liver microsomal stablity: 54.0% (human), 70.1% (rat)